Journal of Materials Chemistry A

ROYAL SOCIETY OF CHEMISTRY

COMMUNICATION

View Article Online
View Journal | View Issue

Cite this: J. Mater. Chem. A, 2025, 13, 24466

Received 7th April 2025
Accepted 10th July 2025

DOI: 10.1039/d5ta02758f

rsc.li/materials-a

Sustainable recovery of perfluoroalkyl acids using a reusable molecular cage†

María Pérez-Ferreiro, [a] Quinn M. Gallagher, [b] Michael A. Webb, [b] Alejandro Criado *[a] and Jesús Mosquera *[a]

Perfluoroalkyl acids (PFAAs) are widely used surfactants valued for their unique physicochemical properties; however, their environmental persistence and high production costs present major challenges. Current approaches predominantly focus on remediation, with efficient recovery strategies remaining underdeveloped. Here, we introduce a simple and sustainable method for PFAA recovery using a water-soluble organic molecular cage. Each cage molecule selectively induces the precipitation of approximately 19 PFAA molecules from complex media. Owing to the exceptional stability of the cage, both the cage and the PFAAs can be fully regenerated *via* a low-energy, solvent-free acid treatment. The cage is synthesized through a scalable, chromatography-free process and supports a closed-loop recovery cycle. Recovery efficiency remains high across three cycles, with 94% of PFOA recovered by mass balance, confirming the robustness and practicality of the system. This strategy offers a cost-effective and environmentally responsible solution, simultaneously addressing PFAA contamination and resource recovery.

Introduction

Perfluoroalkyl acids (PFAAs) constitute a unique class of synthetic surfactants characterized by exceptional chemical stability, surface activity, and thermal resistance, making them indispensable across diverse industrial applications.[1,2] Their utility spans advanced photolithography,[3] semiconductor manufacturing,[4] and the synthesis of high-performance fluoropolymers[5] such as polytetrafluoroethylene (PTFE). Among them, perfluorooctanoic acid (PFOA) has been widely used as a critical emulsifier in PTFE polymerization, facilitating the production of durable coatings, electronic components, and aerospace materials.[6]

However, the environmental persistence[7] and bioaccumulative nature[8] of PFAAs have raised significant concerns regarding their potential risks to human health and ecosystems.[9,10] Their resistance to degradation has led to widespread contamination of water sources, soil, and biota, with emerging evidence linking chronic exposure to adverse health effects.[11] Consequently, several analytical techniques have been developed to detect and quantify PFAAs even at trace levels.[12,13] Despite these concerns, the global market for PFAAs remains strong, with PFOA alone currently valued at $9.74 billion and projected to exceed $12 billion by 2028,[14] underscoring its continued industrial relevance and the challenges associated with phasing out its use.

The research community is actively working to address the challenges posed by PFAAs through two main approaches: (i) developing alternative surfactants[15] and (ii) removing PFAAs from contaminated environments.[16] Replacing PFAAs is particularly challenging due to their exceptional features, all of which stem from the strength of the carbon–fluorine bond in their structure.[2]

Various remediation strategies, including advanced oxidation processes,[17] adsorption technologies,[18,19] and bioremediation,[20,21] are being explored to mitigate PFAA contamination. Among these, molecular cages—synthetic macromolecules with well-defined cavities capable of precise molecular recognition[22–24]—have emerged as promising materials for addressing technological challenges.[25–27] Recent studies have demonstrated their potential for the removal of PFAAs, offering an approach to remediation.[28–31]

However, given that PFAAs are costly to produce—ranging from 100 to 1000 times more per unit volume than conventional hydrocarbon surfactants[32]—remediation methods that lead to irreversible destruction or sequestration are far from ideal, as they result in resource loss and increased economic burden. This highlights the urgent need for recovery strategies that

[a]CICA-Centro Interdisciplinar de Química e Bioloxía, Facultade de Ciencias, Universidade da Coruña, Campus de Elviña, 15071, A Coruña, Spain. E-mail: j.mosquera1@udc.es; a.criado@udc.es

[b]Department of Chemical and Biological Engineering, Princeton University, Princeton, NJ 08544, USA

† Electronic supplementary information (ESI) available. See DOI: https://doi.org/10.1039/d5ta02758f

enable the reuse of PFAAs while minimizing environmental impact.

In this context, we present a recovery technology for PFAAs based on a fully organic molecular cage, **p-A_2B_3**, which can be synthesized in just two steps with high yield, without the need for chromatographic purification. This molecular cage facilitates the efficient recovery of PFAAs from complex aqueous mixtures through a streamlined, two-step process involving the simple separation of a solid from the liquid phase. Notably, the method operates without organic solvents and ensures the quantitative recovery of both the cage and high-purity PFAAs.

Results and discussion

Synthesis and characterization of p-A_2B_3

p-A_2B_3 was synthesized following a synthetic methodology reported by our group last year[33] (Fig. 1), which involves: (i) cage formation *via* imine chemistry, (ii) covalent locking through reduction, and (iii) a post-synthetic modification to attach pendant groups to the resulting secondary amines. The first two steps were performed in a one-pot reaction, yielding the intermediate cage **A_2B_3**. Specifically, the condensation of 1,3,5-tris(aminomethyl)-2,4,6-trimethylbenzene (**A**) with bis(4-formylphenyl)phenylamine (**B**) yielded an imine cage, which was subsequently reduced using sodium borohydride and purified by reverse-phase chromatography. The resulting **A_2B_3** is water-soluble only when protonated with hydrochloric or trifluoroacetic acid. Comprehensive characterization of **A_2B_3** was performed using NMR, which exhibited sharp peaks, as well as mass spectrometry (MS) and liquid chromatography-mass spectrometry (LC-MS) (Fig. S6 and S9†).

The final step in **p-A_2B_3** synthesis involved coupling 3-carboxy-*N*,*N*,*N*-trimethylpropan-1-aminium to the cage's amino groups using the coupling agent hexafluorophosphate azabenzotriazole tetramethyl uronium (HATU). This modification introduced six cationic pendants, resulting in a highly charged, water-soluble cage. Unlike its precursor, **p-A_2B_3** exhibits excellent solubility in phosphate-buffered saline (PBS) at neutral pH, enabling solubility in aqueous media at concentrations around 2 mM. As observed in the previously prepared cage using this methodology, ^{1}H-NMR analysis revealed broad peaks in water and dimethyl sulfoxide (DMSO), attributed to restricted rotation caused by the partial double-bond character of amides. To obtain a defined ^{1}H-NMR spectrum, measurements were conducted at 90 °C in DMSO (Fig. S15†). LC-MS and high-resolution MS further confirmed the structure and purity of **p-A_2B_3** (Fig. S11 and S12†).

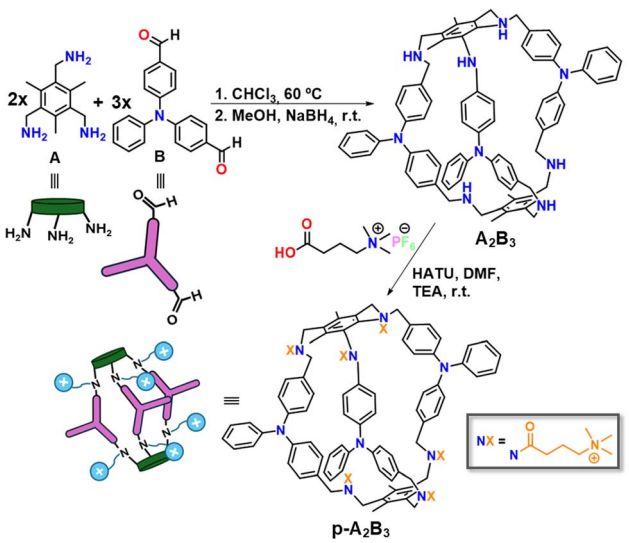

Fig. 1 Synthesis of p-A_2B_3.

Evaluation of p-A_2B_3 interaction with PFOA

To evaluate the ability of **p-A_2B_3** to capture PFAAs, we first conducted titration experiments using PFOA. When an aqueous solution of PFOA (1 mM) was titrated with **p-A_2B_3**, the ^{19}F-NMR signals of PFOA gradually disappeared, accompanied by the formation of a solid precipitate in the NMR tube.

Using sodium tetrafluoroborate as an internal reference, the titration revealed that only 0.05 equivalents of the cage were required to induce complete precipitation of PFOA from the solution. The decrease in PFOA signal intensity exhibited a linear correlation with cage addition, yielding a slope of approximately −19 (Fig. 2a), suggesting that each **p-A_2B_3** molecule, carrying a total charge of +6, associates with 19 anionic PFOA molecules, leading to their precipitation. Given that the internal cavity of **p-A_2B_3** (~1.3 nm)[34] is too small to host 19 PFOA molecules (each ~1 nm in length and ~216 Å^3 in volume), the observed stoichiometry strongly supports an external surface association rather than encapsulation.

To further assess the applicability of this methodology in complex matrices, we conducted the same titration experiment in progressively more intricate media, transitioning from pure water to phosphate-buffered saline (PBS), seawater, and an aqueous solution of Dulbecco's Modified Eagle Medium (DMEM). In both PBS and seawater, precipitation occurred similarly to pure water, with the only difference being a slight increase in the required equivalents of **p-A_2B_3** to achieve complete PFOA precipitation, increasing from 0.05 to 0.09 equivalents (Fig. 2c and d). Finally, the most complex medium that we studied was 10% DMEM solution in water. This is a complex cell culture medium that contains amino acids, vitamins, glucose, inorganic salts, and buffering agents, making it a valuable test medium for evaluating the robustness and real-world applicability of this system. Despite the complexity of the mixture, just 0.09 equivalents of **p-A_2B_3** (Fig. 2e) were again sufficient to precipitate PFOA. These findings confirm that the cage remains effective even in complex mixtures, highlighting its potential for real-world applications.

Exploring the interaction of p-A_2B_3 with other surfactants

To further explore the scope of our system, we examined the interaction of the cage with a series of PFAAs (Fig. S20–S23†), including potassium perfluorohexanesulfonate (PFBS), perfluoroheptanoic acid (PFHpA), potassium nonafluoro-1-butanesulfonate, and perfluoropentanoic acid. These PFAAs

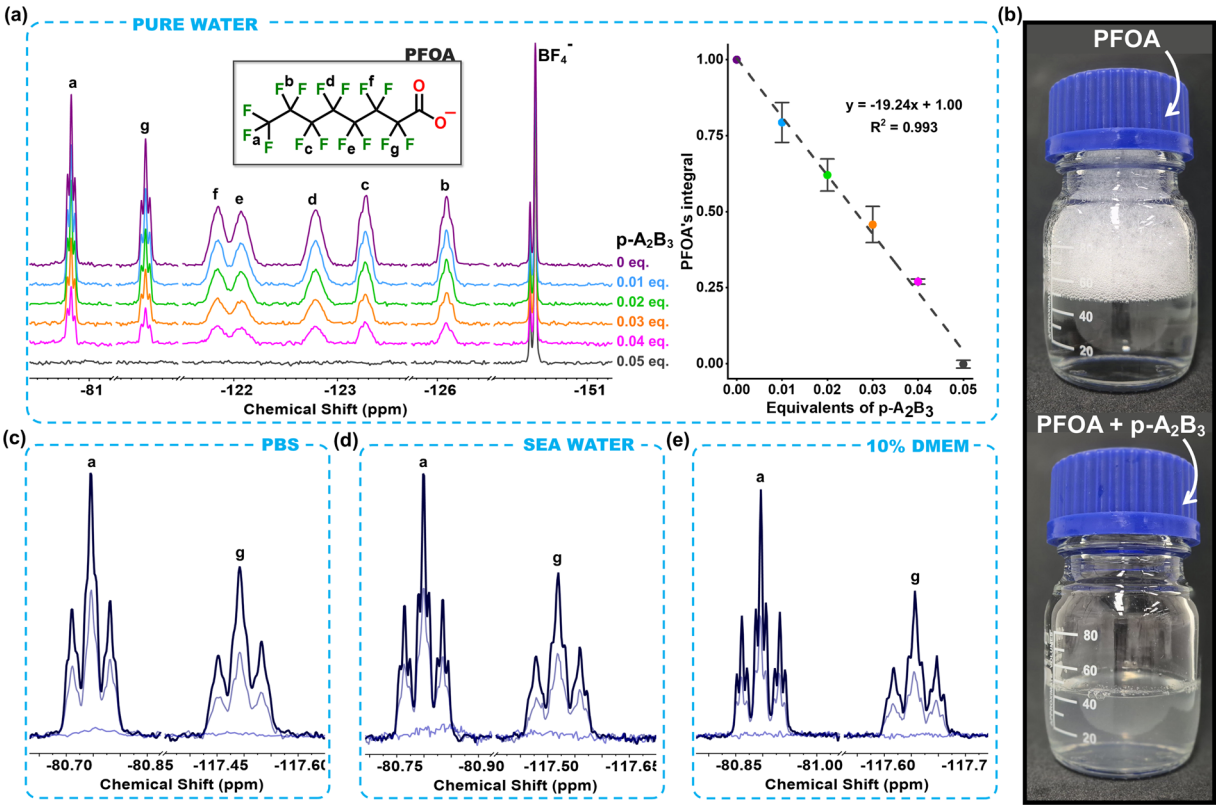

Fig. 2 Evaluation of **p-A_2B_3** interaction with PFOA. (a) ^{19}F-NMR spectra of PFOA titrated with **p-A_2B_3** in D_2O (left) and the corresponding linear fit (right). (b) Photographs of the flask containing PFOA before and after the addition of **p-A_2B_3**, showing the precipitation. ^{19}F-NMR spectra of PFOA in (c) 10 mM PBS solution, (d) seawater, and (e) an aqueous solution enriched with 10% DMEM before and after the addition of **p-A_2B_3** at 0.025 and 0.09 equivalents. The spectra demonstrate the disappearance and effective removal of PFOA, indicating its precipitation upon interaction with **p-A_2B_3**.

vary in both chain length and headgroup chemistry, ranging from sulfonates to carboxylic acids.

Titration experiments, monitored by ^{19}F-NMR using $NaBF_4$ as an internal reference, revealed distinct behavioral differences. A clear correlation emerged between surfactant chain length and the ability of **p-A_2B_3** to induce precipitation. Longer-chain PFAAs, such as PFBS and PFHpA, both featuring hydrophobic tails and distinct head groups—sulfonate (PFBS) and carboxyl (PFHpA)—precipitated upon the addition of 0.05 and 0.03 equivalents of **p-A_2B_3**, respectively. This suggests that **p-A_2B_3** effectively stabilizes aggregates of longer-chain PFAAs, likely due to strong hydrophobic interactions. In contrast, shorter-chain PFAAs, such as potassium nonafluoro-1-butanesulfonate and perfluoropentanoic acid, interact with the cage but do not precipitate. These experiments highlight that the affinity of PFAAs for **p-A_2B_3** is primarily governed by electrostatic interactions. While these compounds do not precipitate, they still interact with **p-A_2B_3**. This lack of precipitation highlights the critical role of chain length in the cage-induced aggregation process.

To examine in more detail the specificity of this phenomenon, we performed ^{1}H NMR titrations in D_2O with hydrophobic anions structurally distinct from the surfactant molecules. Three representative compounds were selected: adenosine, a charged and moderately hydrophobic nucleoside; tryptophan, a zwitterionic and highly hydrophobic amino acid also present in DMEM; and *p*-toluene sulfonate, a negatively charged aromatic sulfonate. None of these molecules precipitated upon the addition of **p-A_2B_3** (Fig. S24–S26†) even when added at ten times the equivalents required for complete PFOA precipitation, indicating high selectivity of the cage towards PFAAs. Furthermore, a mixture of PFOA and *p*-toluene sulfonate was titrated with **p-A_2B_3**, resulting in complete disappearance of PFOA signals due to precipitation while the *p*-toluene sulfonate remained fully in solution (Fig. S27 and S28†). These results confirm the selective precipitation of PFAAs by **p-A_2B_3** in the presence of competing hydrophobic or charged species. Although *p*-toluene sulfonate is known from previous experiments to interact with the cage, this interaction did not interfere with the precipitation of PFOA.

Exploring the recovery of PFOA and p-A_2B_3 from complex media

As mentioned in the introduction, current methodologies for addressing PFAAs prioritize remediation over recovery, largely due to the complexity of adsorbent recovery protocols. Typically, this process involves washing the adsorbent with a saturated NaCl–MeOH solution.[28,29] However, this approach results in the

surfactant becoming highly diluted in the organic solvent and contaminated with salts, significantly limiting its reusability.

Two additional features make this cage particularly appealing: its high solubility in water (~2 mM) due to the presence of quaternary ammonium cationic pendants and its remarkable chemical stability due to its pure organic nature. Based on these observations, we investigated whether the PFAA/cage complex could be disrupted by the simple addition of a strong acid diluted in water. Under these conditions, the protonated PFAAs should lose their affinity for the cage due to their neutralization and remain insoluble in water, as reported for their protonated states.[35] In contrast, the cage should associate with the anions of the acid and regain its water solubility (Fig. 3).

To test our hypothesis, a 10% DMEM solution in D_2O (5 mL) was contaminated with 1 mM PFOA and treated with 0.1 equivalents of the cage to induce the precipitation of the PFOA–cage complex (Fig. 3a – Step 1). The resulting solid was isolated, and the liquid phase was analyzed by ^{19}F-NMR, confirming the absence of PFOA peaks (Fig. 3c). Then, the solid was treated with 5 mL of HCl (1 M) (Fig. 3a – Step 2). Upon acid addition, the solution turned yellowish, indicating the dissolution of the cage while maintaining a white precipitate. The precipitated PFOA was then collected and recovered in its original commercial form as a protonated compound. The purity of the surfactant and the cage was validated *via* ^{19}F-NMR and ^{1}H-NMR for PFOA and **p-A_2B_3**, as well as HPLC for the latter (Fig. S29–S38†).

In the case of PFOA, ^{19}F-NMR confirmed the identity of the recovered surfactant, while the ^{1}H-NMR spectra showed no detectable signals from any DMEM components, indicating high chemical purity and the absence of co-extracted organic molecules (Fig. S36†). On the other hand, the purity of the recovered cage was specifically evaluated using ^{19}F-NMR, which showed no detectable signals of PFOA, confirming the absence of this surfactant (Fig. 3e). Additionally, ^{1}H-NMR was performed to check for possible contamination from components of the DMEM medium (Fig. S33†). However, the inherent broadness of the cage's ^{1}H-NMR spectrum limits the ability to conclusively exclude minor impurities from the medium. To complement this analysis, reverse-phase HPLC was employed, revealing a single, well-defined peak corresponding to the cage (Fig. 3f). Together, these results confirm the high purity of the recovered cage.

Notably, the entire process was conducted exclusively in water, eliminating the need for organic solvents. This renders the method environmentally friendly, cost-effective, and scalable. This same protocol was carried out with PFHpA, and the results mimic those obtained for PFOA. Sulfonate-based PFAAS

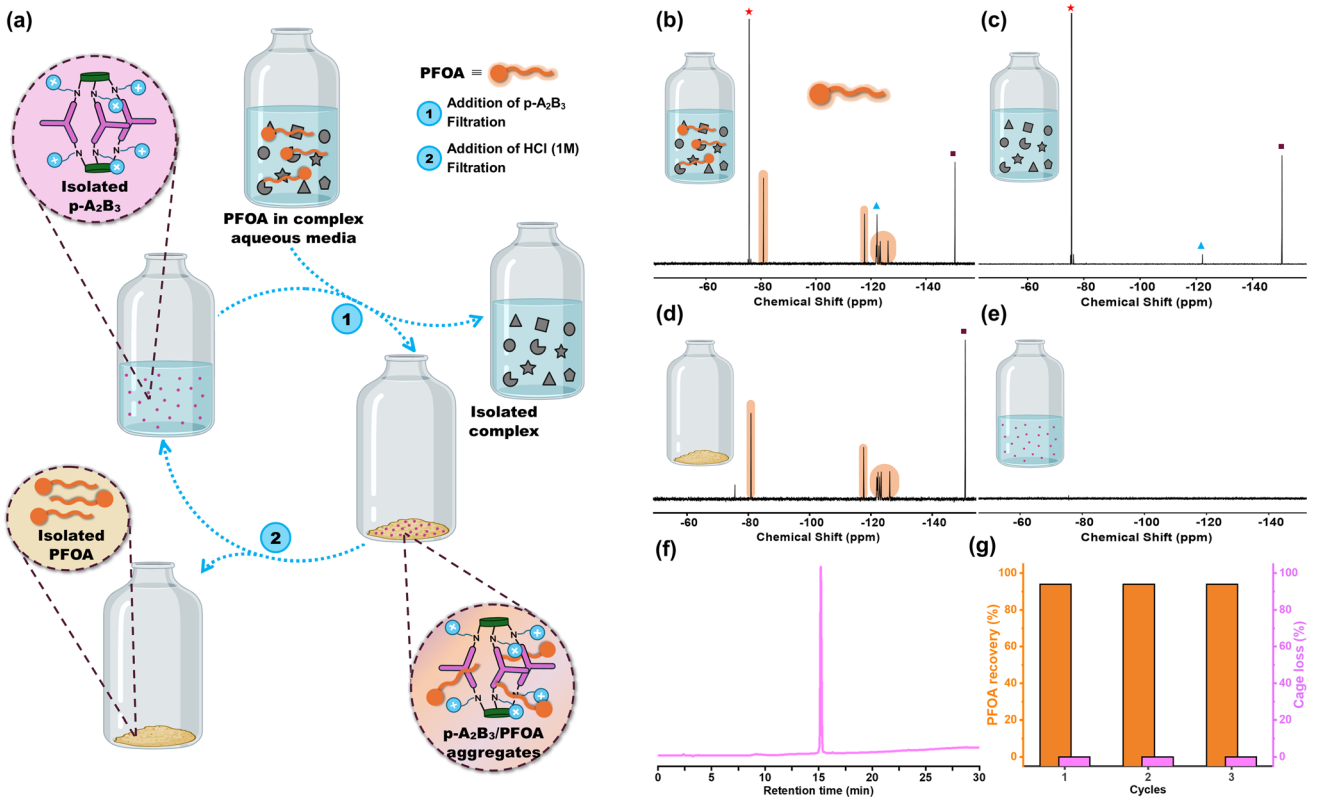

Fig. 3 (a) Schematic representation of the recovery process for both PFOA and the cage. (b) ^{19}F-NMR spectrum of 10% DMEM contaminated with 1 mM PFOA, where the star and triangle indicate impurities from DMEM and PFOA, respectively, and the square represents the internal standard signal ($NaBF_4$). (c) ^{19}F-NMR spectrum after the addition of 0.09 equivalents of **p-A_2B_3**, showing the complete removal of PFOA from the solution. (d) ^{19}F-NMR spectrum of recovered PFOA after solubilization in basic D_2O. (e) ^{19}F-NMR spectrum of the recovered cage, confirming the absence of PFOA. (f) Obtained HPLC chromatogram for the recovered **p-A_2B_3**, confirming its purity and absence of degradation. (g) Bar chart showing the recovery efficiency of PFOA over three consecutive regeneration cycles using **p-A_2B_3**, calculated by gravimetric analysis.

such as PFBS could also be recovered using our cage system, although a different approach was required. Unlike carboxylates, sulfonate anions are extremely weak bases and resist protonation even under strongly acidic conditions, making acid-induced precipitation ineffective. To address this, we employed an alternative strategy inspired by a previously reported method, in which tetrabutylammonium sulfate (TBA_2SO_4) was used to selectively precipitate the cage from organic media.[30] This approach enabled efficient separation of the cage from the sulfonated surfactant by disrupting the hydrophobic interactions between them, allowing the PFBS to remain in solution while the cage was recovered by precipitation (Fig. S39†).

To evaluate the reusability of the cage, we performed three full cycles consisting of PFOA precipitation, recovery of both PFOA and **p-A_2B_3**, and reuse of the recovered cage in a new PFOA solution. In each case, the recovered cage was directly added to a 1 mM PFOA solution in 10% DMEM, where it effectively induced precipitation. Gravimetric analysis was carried out after each cycle to confirm that the cage's efficiency was preserved. Notably, 94% of the initial PFOA was recovered even in the third cycle, demonstrating that the cage maintains its precipitation ability over multiple uses (Fig. 3g).

Finally, we assessed whether the synthesis of **p-A_2B_3** could be simplified and performed on the gram scale to make this technology suitable for industrial application. To accomplish this, we conducted a detailed analysis of the crude reaction mixture after reduction. Mass spectrometry confirmed the main impurity as an amine–borane complex, in agreement with literature reports.[36] To eliminate this impurity, the crude was stirred overnight in a solution of 150 mL MeOH and 15 mL concentrated HCl (37%). HPLC analysis confirmed its complete removal, leaving only the pure product (Fig. S9†). Additionally, purification of **p-A_2B_3** by HPLC can be replaced by washing the crude product with 1 M KOH and water to eliminate HOAt, ensuring a clean final product (Fig. S16†). These optimizations allow for a streamlined, scalable synthesis with 94% yield, making it highly suitable for industrial applications.

Experimental section

General methods

HPLC purification was carried out using a Phenomenex Luna Omega Polar C18 column (5 μm, size: 250 × 10 mm) with Phase A/Phase B gradients (Phase A: H_2O with 0.1% trifluoroacetic acid; Phase B: Acetonitrile with 0.1% trifluoroacetic acid). Proton nuclear magnetic resonance (^{1}H-NMR), carbon nuclear magnetic resonance (^{13}C-NMR) and fluorine nuclear magnetic resonance (^{19}F-NMR) spectra were measured on Bruker AVANCE III HD 300 Nuclear Magnetic Resonance spectrometer or a Bruker AVANCE III HD 500 Nuclear Magnetic Resonance spectrometer and were referenced relating to residual proton resonances in $CDCl_3$ (at δ 7.24 ppm), D_2O (at δ 4.79 ppm) and CD_3SO (at δ 2.50 ppm). Carbons are referenced relating to residual carbon resonances in $CDCl_3$ (at δ 77.06 ppm). ^{1}H-NMR splitting patterns are assigned as singlet (s), doublet (d), triplet (t) or quartet (q). Splitting patterns that could not be readily interpreted are designated as multiplet (m). All chemical shift (δ) values are given in parts per million. All coupling constants are quoted in Hz. All ^{13}C and ^{19}F spectra are proton decoupled unless otherwise stated. Mass spectra were recorded in positive mode using an electrospray ionization technique (ESI) in a LC-Q-q-TOF Applied Biosystems QStar Elite mass spectrometer located at the Research Support Services, SAI (Servizos de Apoio á Investigación) of the University of A Coruña. The predicted mass spectra were calculated using mMass Software, version 5.5.0. ^{19}F-NMR for the titrations of PFAAs were measured on Bruker AVANCE III HD 300 Nuclear Magnetic Resonance spectrometer, with a scan number of 200. Every titration was done using a concentration of 1 mM of surfactant and 0.5 mM of $NaBF_4$, unless stated otherwise. For each addition of p-A_2B_3, the corresponding equivalents were added from a concentrated stock in D_2O.

Synthesis of A_2B_3. The synthesis of (2,4,6-trimethylbenzene-1,3,5-triyl)trimethana-mine (**A**), was carried out in two steps based on protocol described in literature.[37] A solution of (2,4,6-trimethylbenzene-1,3,5-triyl)trimethanamine **A** (48.2 mg, 0.23 mmol, 2.1 eq.) and tris(4-formylphenyl)amine **B** (100 mg, 0.33 mmol, 3 eq.) dissolved in $CHCl_3$ (50 mL) was heated at 60 °C for 2 days. Reaction was allowed to cool to room temperature and 50 mL of MeOH and 100 mg of $NaBH_4$ were added. The solution was left stirring at room temperature overnight. Then, the solvent was removed under vacuum and the resulting solid was washed one time with NaOH 1 M, and two times with pure water. Then, it was purified by HPLC, using Phase A/Phase B gradients, from 95% to 5% of A, with Phenomenex Luna Omega Polar C18 column (5 μm, 100 Å, 250 × 10 mm), in 30 minutes. The final product (89 mg, 67%) was obtained as a fluffy white solid.

Synthesis of p-A_2B_3. Previous to the modification of **A_2B_3**, the 3-carboxy-*N*,*N*,*N*-trimethylpropan-1-aminium chloride that was commercially available from BLDPharm was treated with $NaPF_6$ in order to exchange the counterion because it was observed that this exchange does favor the reaction. Thus, 3-carboxy-*N*,*N*,*N*-trimethylpropan-1-aminium chloride was dissolved in water, where a solution of $NaPF_6$ was added, causing the precipitation of the salt, that was then dried. 3-Carboxy-*N*,*N*,*N*-trimethylpropan-1-aminium hexafluorophosphate (142.9 mg, 12 eq.), HATU (187.1 mg, 12 eq.) and triethylamine (171 μL, 30 eq.) were dissolved in 1 mL of DMF and stirred at room temperature until the apparition of yellowish color (around 5 min). Then, **A_2B_3** was added to the mixture (60.0 mg, 1 eq.) and the resulting yellow solution was left stirring at room temperature for 1 h. After that time, DMF was removed under vacuum and the resulting sticky solid was purified by HPLC using Phase A/Phase B gradients, from 95% to 5% of A, with a Phenomenex Luna Omega Polar C18 column, in 30 minutes. The final product (69 mg, 64%) was obtained as a white solid.

Scaling up protocol

A solution of (2,4,6-trimethylbenzene-1,3,5-triyl) trimethanamine **A** (482 mg, 2.32 mmol, 2.1 eq.) and tris(4-formylphenyl)amine **B** (1 g, 3.32 mmol, 3 eq.) dissolved in

$CHCl_3$ (500 mL) was heated at 60 °C for 2 days. Reaction was allowed to cool to room temperature and 500 mL of MeOH and 1 g of $NaBH_4$ were added. The solution was left stirring at room temperature overnight. Then, the solvent was removed under vacuum and the resulting solid was washed one time with NaOH 1 M, and two times with pure water. Then, 150 mL of MeOH and 15 mL of HCl (37%) were added to the resulting solid, and the orange mixture was left stirring overnight. The solution was concentrated, and the resulting solid was dried. The final compound was obtained as a whitish solid, in 96%.

3-Carboxy-*N*,*N*,*N*-trimethylpropan-1-aminium hexafluorophosphate (572 mg, 12 eq.), HATU (497 mg, 12 eq.) and triethylamine (684 μL, 30 eq.) were dissolved in 5 mL of DMF and stirred at room temperature until the apparition of yellowish color (around 5 min). Then, $\mathbf{A_2B_3}$ was added to the mixture (200 mg, 1 eq.) and the resulting yellow solution was left stirring at room temperature for 1 h. After that time, DMF was removed under vacuum and the resulting sticky solid was washed once with KOH (1 M) and twice with pure water. The resulting white solid was dried, the product was obtained in 92% yield. Once the cage was synthesized, two different routes were explored to make it functional, as the $[PF_6]^-$ counterions are too hydrophobic to ensure water solubility. (i) Purification by HPLC using H_2O/ACN (0.1% TFA). (ii) Counterion exchange using tetrabutylammonium sulphate. $[\mathbf{p\text{-}A_2B_3}]^{6+}$ $6[PF_6]^-$ can be dissolved in acetonitrile and then, stoichiometric amount of tetrabutylammonium sulphate is added, leading to the precipitation of $[\mathbf{p\text{-}A_2B_3}]^{6+}$ $3[SO_4]^{2-}$ that can be directly used.

Conclusions

In summary, we report a scalable, sustainable, and highly selective method for the recovery of perfluoroalkyl acids (PFAAs) using the cationic organic molecular cage $\mathbf{p\text{-}A_2B_3}$. Synthesized *via* a high-yield, chromatography-free process, each $\mathbf{p\text{-}A_2B_3}$ efficiently captures and precipitates around 20 molecules of PFAAs—including PFOA—through synergistic electrostatic and hydrophobic interactions. The cage demonstrates robust performance across diverse aqueous environments, including phosphate-buffered saline, seawater, and complex biological media. Unlike conventional sequestration strategies, this approach enables the recovery of PFAAs in their commercial form through a simple, solvent-free acid treatment, allowing full regeneration of both the cage and the guest molecules. This not only minimizes chemical waste and energy consumption but also aligns with circular economic principles.

Recovery experiments conducted over three consecutive cycles showed consistent performance, with 94% of PFOA recovered by mass balance in each cycle. This highlights the reliability of the process and the ability of the cage to retain its efficacy upon reuse, supporting its potential for large-scale environmental remediation and industrial deployment. Based on a comparative analysis presented in Table S3,† $\mathbf{p\text{-}A_2B_3}$ exhibits the highest PFAA loading capacity reported to date, capturing approximately 19 PFAA molecules per cage. Moreover, it is the only system that enables recovery of both the cage and the PFAAs in their pure forms without the use of organic solvents. This highlights the unique combination of efficiency, sustainability, and operational simplicity of $\mathbf{p\text{-}A_2B_3}$, making it especially attractive for scalable environmental remediation efforts.

Data availability

The data supporting this article have been included as part of the ESI,† such as detailed experimental procedures and characterization.

Author contributions

J. M. and A. C. conceived the project and designed the experiments. M. A. W. and M. P.-F. assisted with the experimental analysis. J. M., A. C., M. P.-F., M. A. W., and Q. M. G. co-wrote the manuscript. All authors contributed to discussing and analyzing the results.

Conflicts of interest

There are no conflicts to declare.

Acknowledgements

This research was supported by the Xunta de Galicia under Project Proxectos de Excelencia (No. ED431F 2022/02). A. C. (RYC2020-030183-I and PID2021-127002NA-I00) and J. M. (RYC2019-027842-I) acknowledges financial support by their Grants RYC2020-030183-I funded by MCIN/AEI/10.13039/501100011033 and "ESF Investing in your future". M.A.W. acknowledges support from the National Science Foundation under Grant No. 2237470.

Notes and references

1 J. Glüge, M. Scheringer, I. T. Cousins, J. C. DeWitt, G. Goldenman, D. Herzke, R. Lohmann, C. A. Ng, X. Trier and Z. Wang, *Environ. Sci.: Processes Impacts*, 2020, **22**, 2345–2373.
2 S. C. E. Leung, D. Wanninayake, D. Chen, N.-T. Nguyen and Q. Li, *Sci. Total Environ.*, 2023, **905**, 166764.
3 Y. Liu, D. Wang, Q. Wang and W. Kang, *Small Methods*, 2024, **8**, 2400112.
4 World Intellectual Property Organization, *WO2013119976A1*, 2013.
5 B. Ameduri, *Chem.–Eur. J.*, 2018, **24**, 18830–18841.
6 G. J. Puts, P. Crouse and B. M. Ameduri, *Chem. Rev.*, 2019, **119**, 1763–1805.
7 X. C. Hu, D. Q. Andrews, A. B. Lindstrom, T. A. Bruton, L. A. Schaider, P. Grandjean, R. Lohmann, C. C. Carignan, A. Blum, S. A. Balan, C. P. Higgins and E. M. Sunderland, *Environ. Sci. Technol. Lett.*, 2016, **3**, 344–350.
8 Y. Shi, R. Vestergren, Z. Zhou, X. Song, L. Xu, Y. Liang and Y. Cai, *Environ. Sci. Technol.*, 2015, **49**, 14156–14165.

9 D. Ackerman Grunfeld, D. Gilbert, J. Hou, A. M. Jones, M. J. Lee, T. C. G. Kibbey and D. M. O'Carroll, *Nat. Geosci.*, 2024, **17**, 340–346.
10 M. Ateia and M. Scheringer, *Science*, 2024, **385**, 256–258.
11 S. E. Fenton, A. Ducatman, A. Boobis, J. C. DeWitt, C. Lau, C. Ng, J. S. Smith and S. M. Roberts, *Environ. Toxicol. Chem.*, 2021, **40**, 606–630.
12 A. L. B. Forster, T. C. Geiger, G. O. Pansari, P. T. Justen and S. D. Richardson, *Water Res.*, 2024, **256**, 121570.
13 A. Concellón, J. Castro-Esteban and T. M. Swager, *J. Am. Chem. Soc.*, 2023, **145**, 11420–11430.
14 Perfluorooctanoic acid global market value 2028, **https://www.statista.com/statistics/1454360/global-perfluorooctanoic-acid-market-value/**, accessed March 12, 2025.
15 R. Figuière, L. T. Miaz, E. Savvidou and I. T. Cousins, *Environ. Sci. Technol.*, 2025, **59**, 2031–2042.
16 Z. Abbasian Chaleshtari and R. Foudazi, *ACS EST Water*, 2022, **2**, 2258–2272.
17 T. A. Bruton and D. L. Sedlak, *Environ. Sci. Technol.*, 2017, **51**, 13878–13885.
18 M. Sörengård, E. Östblom, S. Köhler and L. Ahrens, *J. Environ. Chem. Eng.*, 2020, **8**, 103744.
19 C. A. Clark, K. N. Heck, C. D. Powell and M. S. Wong, *ACS Sustainable Chem. Eng.*, 2019, **7**, 6619–6628.
20 C. M. Smorada, M. W. Sima and P. R. Jaffé, *Curr. Opin. Biotechnol.*, 2024, **88**, 103170.
21 M. Hu and C. Scott, *Appl. Environ. Microbiol.*, 2024, **90**, e00157–24.
22 G. Li, T. K. Ronson, R. Lavendomme, Z. Huang, C. Fuertes-Espinosa, D. Zhang and J. R. Nitschke, *Chem*, 2023, **9**, 1549–1561.
23 G. Montà-González, F. Sancenón, R. Martínez-Máñez and V. Martí-Centelles, *Chem. Rev.*, 2022, **122**, 13636–13708.
24 S. Ruiz-Relaño, D. Nam, J. Albalad, A. Cortés-Martínez, J. Juanhuix, I. Imaz and D. Maspoch, *J. Am. Chem. Soc.*, 2024, **146**, 26603–26608.
25 J. Zhao, K. Zeng, W.-T. Dou, X. Zhao, W. Wang, X. Shi, X. Li, J. Fang, X. Qian, H.-B. Yang and L. Xu, *Adv. Funct. Mater.*, 2025, **35**, 2413920.
26 O. Yanshyna, M. J. Białek, O. V. Chashchikhin and R. Klajn, *Commun. Chem.*, 2022, **5**, 1–12.
27 A. Fakim, B. I. Maatouk, B. Maiti, A. Dey, S. H. Alotaiby, B. A. Moosa, W. Lin and N. M. Khashab, *Adv. Healthcare Mater.*, 2024, **13**, 2401117.
28 Y. He, J. Zhou, Y. Li, Y.-D. Yang, J. L. Sessler and X. Chi, *J. Am. Chem. Soc.*, 2024, **146**, 6225–6230.
29 K. R. Sanchez-Lievanos, D. Zhang, S. M. Simpson, M. K. Wijayahena, G. Rizzo, J. M. N. Aguilar, L. M. Abaya, J. M. Dovi, H. I. Sirotkin, M. R. Crawley, T. R. Cook and D. S. Aga, *ACS EST Eng.*, 2025, **5**, 701–713.
30 M. D. Bairagya, P. S. Ntipouna, N. K. Stewart and N. Elgrishi, *Chem. Commun.*, 2024, **60**, 11084–11087.
31 D. Camdzic, H. K. Welgama, M. R. Crawley, A. Avasthi, T. R. Cook and D. S. Aga, *ACS Appl. Eng. Mater.*, 2024, **2**, 87–95.
32 J. Glüge, M. Scheringer, I. T. Cousins, J. C. DeWitt, G. Goldenman, D. Herzke, A. B. Lindstrom, R. Lohmann, C. A. Ng, X. Trier and Z. Wang, *Environ. Sci.:Processes Impacts*, 2020, **22**, 2345–2373.
33 M. Pérez-Ferreiro, Q. M. Gallagher, A. B. León, M. A. Webb, A. Criado and J. Mosquera, *Chem. Mater.*, 2024, **36**, 8920–8928.
34 K. Acharyya and P. S. Mukherjee, *Chem. Commun.*, 2014, **50**, 15788–15791.
35 H. Canada, Perfluorooctanoic Acid (PFOA) in Drinking Water, **https://www.canada.ca/en/health-canada/programs/consultation-perfluorooctanoic-acid-pfoa-in-drinking-water/document.html**, accessed March 14, 2025.
36 X. Liu and R. Warmuth, *Nat. Protoc.*, 2007, **2**, 1288–1296.
37 R. L. Greenaway, V. Santolini, M. J. Bennison, B. M. Alston, C. J. Pugh, M. A. Little, M. Miklitz, E. G. B. Eden-Rump, R. Clowes, A. Shakil, H. J. Cuthbertson, H. Armstrong, M. E. Briggs, K. E. Jelfs and A. I. Cooper, *Nat. Commun.*, 2018, **9**, 2849.

